Desalination and Water Treatment
www.deswater.com
doi: 10.1080/19443994.2013.855886

53 (2015) 1641–1652
February

Taylor & Francis
Taylor & Francis Group

Pb^{2+} adsorption onto collagen/cellulose hydrogel beads from aqueous solution: kinetic, isothermal, and thermodynamic analyses

Jilei Wang, Ligang Wei*, Yingchong Ma, Kunlan Li*, Minghui Li, Ningning Ma, Kun Feng, Yingqi Wang

School of Light Industry and Chemical Engineering, Dalian Polytechnic University, Dalian 116034, China
Tel. +86 411 8632 3726; emails: wei_ligang@hotmail.com, likl@dlpu.edu.cn

Received 19 May 2013; Accepted 7 October 2013

ABSTRACT

The removal of Pb^{2+} ions from aqueous solutions using collagen/cellulose hydrogel beads (CCHBs) was investigated using batch adsorption experiments. The results indicate that Pb^{2+} adsorption capacity for the CCHBs is obviously higher than that for the cellulose hydrogel beads (CHBs). The maximum adsorption capacity of Pb^{2+} is at pH 4.2 for the prepared biosorbents. The co-anions slightly influence Pb^{2+} adsorption, whereas the adsorption capacity of Pb^{2+} remains at a high level during the competitive adsorption of heavy metal ions. The behaviors of Pb^{2+} adsorption onto the prepared biosorbents were further analyzed using kinetics, isotherm, and thermodynamics. The overall kinetic data can be adequately explained by a pseudo-second-order model, and Pb^{2+} adsorption is controlled by multiple diffusion mechanism. Pb^{2+} adsorption is described well using the Langmuir model. Thermodynamic evaluations show a spontaneous and endothermic Pb^{2+} adsorption. The entropy for the CCHBs is higher than that for the CHBs and decreases with increasing collagen/cellulose mass ratio from 1:1 to 3:1. This phenomenon indicates that blending collagen in hydrogels changes the interaction or distribution of biopolymers, thereby greatly influencing Pb^{2+} adsorption.

Keywords: Collagen; Cellulose; Hydrogel beads; Pb^{2+}; Adsorption

1. Introduction

Wastewater-containing heavy metals discharged from industries have drawn attention because of its toxic effects on human beings and other living things. Lead ion (Pb^{2+}) is one of the primary pollutants that should be treated [1,2]. Wastewater-containing Pb^{2+} is mainly from the electrical industry and manufacturers of fungicides as well as anti-fouling paints. Conventional approaches, such as chemical precipitation, membrane separation, ion exchange, evaporation, electrolysis, and reverse osmosis, among others, have been used to remove Pb^{2+} from solutions. These methods are often costly, have low efficiency, entails sludge disposal and are inapplicable to a wide range of pollutants [3,4]. Adsorption is advantageous over conventional solvent extraction because of its reduced use of solvents, minimal cost as a result of low consumption of reagents, safety with respect to hazardous solvents, and ease of automation [5]. Various kinds of biopolymers have been prepared as adsorbents to remove Pb^{2+} from wastewater [6–14].

*Corresponding authors.

Collagen, the most abundant triple-helix-structured animal protein, mainly exists in the skin, tendon, cartilage, and other connective tissues of animals and exhibits excellent hydrophilic ability as well as swelling capacity [15]. In China, collagen-rich leather wastes reach 1.4 million tons annually, resulting in environmental pollution and wastage of valuable collagen source. The amino groups in the collagen structure become binding sites by chelating with Pb^{2+} [16]. However, the collagen hardly dissolves in conventional solvents, limiting its application. Ionic liquid (IL), as an environmentally friendly solvent, has been extensively examined. 1-butyl-3-methylimidazolium chloride ([C_4mim]Cl) dissolves collagen to obtain a homogeneous solution by breaking the hydrogen and ionic bonds in collagen macromolecules [17]. Hydrogen bonds can be rebuilt between collagen chains after adding antisolvent water into the obtained solution. The triple-helical structure of collagen can be partly reserved during dissolution and regeneration.

[C_4mim]Cl dissolves cellulose [18], which can be regenerated from the IL–cellulose solution by adding water. IL can be recovered through vacuum evaporation. Interestingly, cellulose/collagen composite films can be prepared by dissolving collagen and cellulose using IL [19]. Strong interactions and good compatibility exist between collagen and cellulose in the film. Polymers exhibit the strongest interactions at a mixing mass ratio of 1:1. The blend films possess better mechanical and water absorption properties than those made of single polymers. The hydrogen bond interactions between cellulose and collagen are also found in the bacterial cellulose/collagen composites, resulting in considerable increase in the Young's modulus and tensile strength [20]. IL also participates as pore formers during reconstitution [21]. Thus, preparing collagen/cellulose porous composite materials for Pb^{2+} adsorption is possible.

Hydrogels are defined as three-dimensional cross-linked polymer network structures composed of hydrophilic copolymers [22,23]. Various hydrogel beads made from biopolymers were employed for Pb^{2+} removal to form aqueous solutions because of their high surface area [11,24]. However, to the best of our knowledge, few investigations using collagen/cellulose hydrogel beads (CCHBs) to adsorb Pb^{2+} from aqueous solution have been conducted. The adsorption mechanisms of CCHBs have also been rarely investigated.

In this study, we first prepared CCHBs using [C_4mim]Cl. Bath adsorptions for Pb^{2+} were considered to investigate the effect of contact time, initial pH, initial Pb^{2+} concentration and temperature. The effect on the adsorption of co-anions and competitive adsorption in a multimetal solution was also investigated. Thermodynamic, kinetic, and isothermal analyses for Pb^{2+} adsorption processes using CCHBs were conducted to ascertain the macroscopic adsorption mechanisms. Two common adsorption isotherms (Langmuir and Freundlich), three kinetic models (pseudo-first-order, pseudo-second-order, and intraparticle diffusion equation), and three thermodynamic parameters (ΔG^0, ΔH^0, and ΔS^0) were used to analyze the adsorption process.

2. Materials and methods

2.1. Materials

The microcrystalline cellulose (MCC, DP 238) was supplied by Shanghai Chinaway Pharmaceutical Tech. Co., Ltd., China. The fresh pigskin used was cleaned, freed of hairs, and then washed thrice with NaCl solution (10 mol/L) to remove mineral substances. Sodium sulphate (Na_2SO_4) (8 mol/L) was used to remove lipids. The pelt was subsequently dehydrated by vacuum drying, grounding, and sieving to yield pigskin collagen powder (0.105 to 0.149 mm and ash content <0.3 wt.%). The [C_4mim]Cl used in this study was prepared and purified according to established procedures [25,26]. The MCC, collagen, and [C_4mim]Cl were vacuum-dried for 24 h to avoid interference from air and water.

Pb^{2+} stock solution was prepared by dissolving $Pb(NO_3)_2$ in deionized (DI) water. $PbNO_3$, $Ni(NO_3)_2$, $Zn(NO_3)_2$, and $Cr(NO_3)_3$ were used to obtain a multimetal solution. Sodium chloride and -COONa were employed to prepare a coanion solution. The pH value of the aqueous solution was adjusted using 1 mol/L HCl or 1 mol/L NaOH solution. All chemicals were of reagent-grade purity and purchased from Chengdu Kelong Reagent Co., Ltd., China.

2.2. Preparation of CCHBs

The 6 wt.% collagen/cellulose/[C_4mim]Cl solutions were first prepared at different collagen/cellulose mass ratios and at 373 K under an inert N_2 atmosphere. The obtained solution was added dropwise to DI water using a 1.0-mm wide syringe needle to produce hydrogel beads. The hydrogel beads were collected and thoroughly rinsed with DI water until no chloride ion could be detected using $AgNO_3$. Pure collagen hydrogel beads cannot be prepared using this method because they are very soft and they easily disintegrate into segments. Thus, three kinds of composite hydrogel beads with varying collagen/cellulose mass ratios, namely CCHB1 (1:1), CCHB2 (2:1), and

CCHB3 (3:1), were prepared. Pure cellulose hydrogel beads (CHBs) were also prepared for comparison. Macroscopically, the prepared CCHBs were spherical in shape, with smooth surface, milky white color, and approximately 3.0 mm wide.

2.3. Characterization of hydrogel beads

Zeta potential is an important parameter for analyzing the electrostatic surface interaction in adsorption. The suspensions (containing colloidal fragments from the hydrogel beads) were employed as the samples for zeta potentials analysis. The pH values of the samples were adjusted to a desired level using 0.1 mol/L HCl or 0.1 mol/L NaOH solution. A Zetasizer Nano (ZEN3600, Malvern, U.K.) was used to measure the zeta potentials of the samples. The cross-sections of hydrogel beads were observed using Scanning electron microscope (SEM, JSM-6460LV, JEOL, Japan). The prepared hydrogel beads were first immersed in liquid nitrogen for 30 min, followed by lyophilization in a freeze drier (LGJ–12, Beijing Songyuan Huaxing Technology Development Co. Ltd., China) for 12 h. The specific surface areas of the adsorbents were measured using an Autosorb NOVA2200e volumetric analyzer (Quanta-chrome, USA). The BET (Brunaeur–Emmet–Teller) multipoint method was used to determine the specific surface area. Nitrogen (N_2) gas was used to determine the adsorption isotherms. The volume quantity and proportion of different pore diameters were calculated by the BJH method.

2.4. Batch adsorption experiments

The batch adsorption experiments were conducted in 50-ml conical flasks with ground stoppers and cap to reduce evaporation. They were agitated at 200 rpm in a thermostatic shaking incubator to reach equilibrium. The stocks of adsorbents with a dosage of 0.5 g (water-holding content 90%)/10 mL were immersed in the ion solution. The concentrations of heavy metal ions before and after adsorption were measured using atomic absorption spectroscopy (180-80, Hitachi, Japan).

3. Results and discussion

3.1. Adsorption behavior of Pb^{2+} on prepared hydrogel beads

3.1.1. Effects of pH value

The effects of pH on Pb^{2+} adsorption were investigated by varying the pH value from 1.0 to 6.0 at 293 K, with initial concentration of 4.5 mmol/L and contact time of 360 min (the time required for Pb^{2+} adsorbed and Pb^{2+} in solution to reach equilibrium). The effects of pH value on the equilibrium adsorption capacities (Q_e) of Pb^{2+} are demonstrated in Fig. 1(a). For the prepared biosorbents, Q_e remarkably increased when the pH value increased from 1.0 to 4.2, before it subsequently decreased (Fig. 1(a)). Pb^{2+} adsorptions onto the CHBs and CCHBs were strongly affected by the pH value of the solution. The maximum Q_e was achieved at the initial pH value of 4.2. Similar phenomena have also been reported in various studies using other biosorbents [8–10].

Zeta potentials of hydrogel beads as a function of solution pH are indicated in Fig. 1(b). The isoelectric points (IEPs, zeta potential = 0) of hydrogel beads are observed from the curves at pH 5.2 (CHB), pH 6.2 (CCHB1), pH 6.4 (CCHB2), and pH 7.3 (CCHB3),

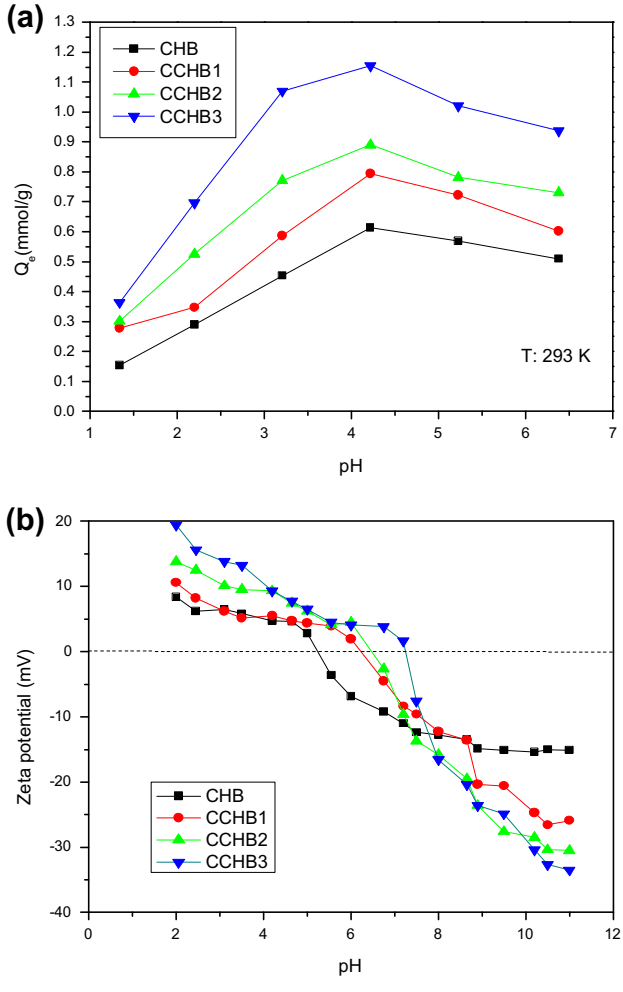

Fig. 1. Effect of the solution pH level on Pb^{2+} adsorption onto the CCHBs and CHBs (a); zeta potentials of hydrogel beads as a function of solution pH (b).

respectively. The IEP values of hydrogel beads increased with increasing collagen content. Below the IEP value, the adsorbent surface is positively charged. In this study, the main adsorption sites for Pb^{2+} are expected to be the nitrogen atoms of the amino groups in collagen and the oxygen atoms of the hydroxyl groups in cellulose. At a low pH level, additional protons are available to protonate adsorption sites that induce electrostatic repulsion of Pb^{2+}, which directly contribute to the reduced amount of binding sites in the adsorbents for adsorption [27,28]. With an increase in pH, the concentration of H^+ decreases, facilitating Pb^{2+} adsorption by the adsorbent. At pH > 4.2, the generation of hydrolyzed species of lead, such as $Pb(OH)^+$ or $Pb(OH)_2$, results in the decrease in the adsorbed amount.

As depicted in Fig. 1(a), Q_e of Pb^{2+} onto the CCHBs is significantly higher than that onto the CHBs. The blending of collagen in the hydrogel matrix provides more binding sites (mainly amino sites) for Pb^{2+} adsorption from the solution. Moreover, the equilibrium adsorption capacity of the composite beads does not increase proportionally with the collagen/cellulose ratio. A small difference between the adsorption capacities of CCHB2 and CCHB1 is found. This phenomenon is also found in the case of Cu^{2+} adsorption (not reported here), possibly because of the change in the interaction between collagen and cellulose molecules with an increase in the collagen/cellulose mass ratio and a decrease in the free amino group in the composite.

3.1.2. Effect of coanions

The effects of common anions in the solution, such as Cl^-, NO_3^-, and COO^-, on Pb^{2+} adsorption were investigated at 293 K under an initial Pb^{2+} concentration of 4.5 mmol/L, pH 4.2, and 360-min contact time. The experimental results are shown in Fig. 2, Where Q'_e is the equilibrium adsorption capacity of Pb^{2+} in the presence of coanions, and Q_e is the equilibrium adsorption capacity of Pb^{2+} in the absence of coanions. Q'_e is slightly lower than Q_e. The results indicate that the presence of coanions in the solution does not considerably affect Pb^{2+} chelating with the active functional groups of the adsorbents.

3.1.3. Competitive adsorption behavior of heavy metal ions

The competitive adsorption of heavy metals, i.e. Pb^{2+}, Ni^{2+}, Zn^{2+}, and Cr^{3+}, in the system was also studied at 293 K under 4.5 mmol/L initial concentration of every heavy metal ion, pH 4.2, and 360 min contact time.

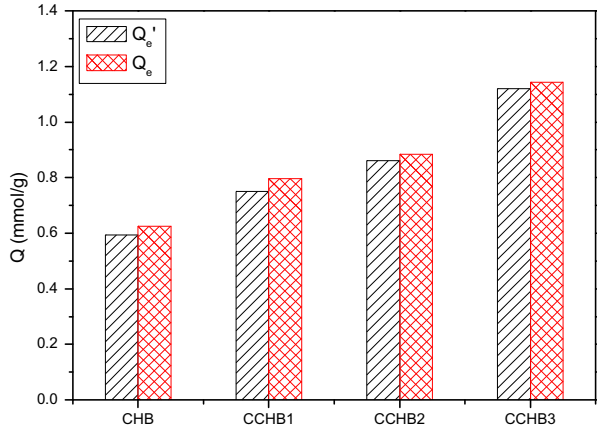

Fig. 2. Effect of co-anions on Pb^{2+} adsorption onto the CCHBs and CHBs.

Fig. 3 illustrates the competitive adsorption between Pb^{2+} and other heavy metal ions (Ni^{2+}, Zn^{2+}, and Cr^{3+}) by prepared hydrogel beads. Other heavy metal ions that contribute to the decrease in Q_e of Pb^{2+} onto the adsorbents are found. The values of Q_e of Pb^{2+} for CCHB3 are 1.144 and 0.875 mmol/g in single- and multimetal systems, respectively. The biosorption order under multimetal ion conditions is $Pb^{2+} > Zn^{2+} > Cr^{3+} > Ni^{2+}$ for the prepared biosorbents. In competitive adsorption, the complex interactions of several factors, such as ionic charge, ionic radius, and electronegativity, affect the biosorption of metal ions on biosorbents [29]. A comparison of the ionic radii

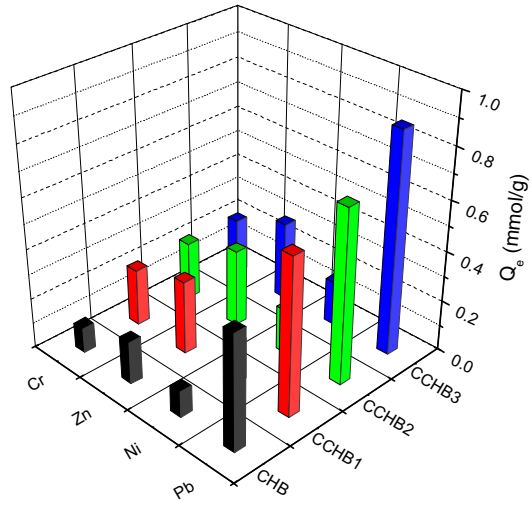

Fig. 3. Competitive adsorption of heavy metal ions from a multi-metal system.

[Pb^{2+} (0.119 Å) > Zn^{2+} (0.074 Å) > Ni^{2+} (0.069 Å) > Cr^{3+} 0.0615 Å)] and electronegativities [Pb^{2+} (2.33) > Ni^{2+} (1.91) > Cr^{3+} (1.66) > Zn^{2+} (1.65)] of the metals elucidates why the affinity of the adsorbent for Pb^{2+} is higher than those for the other metal ions.

3.2. Adsorption kinetics

The adsorption capacities of Pb^{2+} were measured as a function of contact time (ranging from 10 to 720 min) with 4.5 mmol/L initial concentration at pH 4.2 and 293 K (Fig. 4). The adsorption capacities of Pb^{2+} rapidly increased in the first 90 min and then slowly augmented. For the four biosorbents, the adsorption equilibrium could be achieved within 240 min.

The most common models, namely pseudo-first order and pseudo-second order, were used to assume the adsorption kinetics and rate-limiting step, both of which are typically used to study quantitatively the adsorption of heavy metals.

The linear pseudo-first-order model of Lagergren is given as [30]:

$$\log(Q_e - Q_t) = \log\ Q_e - \frac{k_1}{2.303}t \quad (1)$$

where Q_e and Q_t are the amounts (mmol/g) of Pb^{2+} absorbed onto CHB and CCHB at equilibrium and at time t, respectively, and k_1 is the rate constant of the first-order adsorption (min^{-1}). The slopes and intercepts of the plots of $\log(Q_e - Q_t)$ against t (Fig. 5) were used to determine the first-order rate constant k_1, correlation coefficients r, and equilibrium adsorption density $Q_{e,1}$. From Table 1, the calculated $Q_{e,1}$ of the pseudo-first order is much smaller than the experimental value (Q_e) (0.334 mmol/g vs. 0.625 mmol/g, 0.513 mmol/g vs. 0.797 mmol/g, 0.742 mmol/g vs. 0.884 mmol/g, and 0.979 mmol/g vs. 1.144 mmol/g), which may contribute to the existence of a boundary layer or the mass transfer resistance from outside at the beginning of adsorption [31]. In many instances, the first-order equation was only suitable in the initial stages of the adsorption process [32].

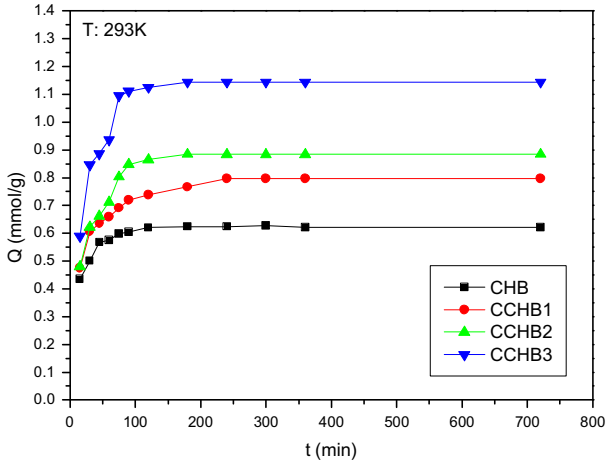

Fig. 4. Pb^{2+} adsorption by the prepared adsorbents as a function of contact time.

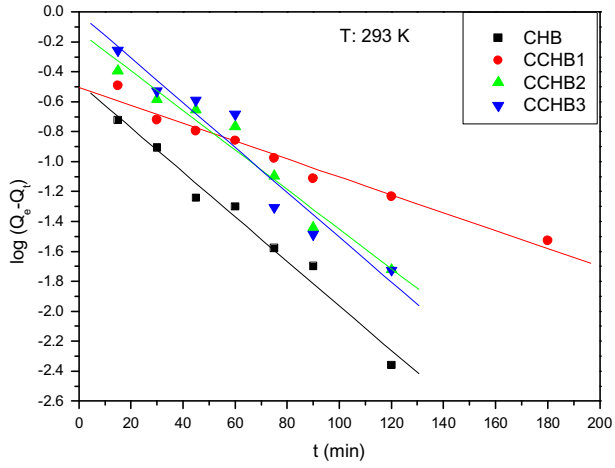

Fig. 5. Pseudo-first-order plot for Pb^{2+} adsorption onto the CCHBs and CHBs.

The linear pseudo-second-order model can be expressed as [33]:

$$\frac{t}{Q_t} = \frac{1}{k_2 Q_e^2} + \frac{t}{Q_e} \quad (2)$$

where k_2 is the rate constant of the second-order adsorption (g/mmol min). The plot of t/Q_t vs. t (Fig. 6) yields very good straight lines for different initial lead concentrations. Thus, they were used to determine the rate constant k_2, correlation coefficient r, and equilibrium adsorption density $Q_{e,2}$. Table 1 lists the calculated results obtained from the first- and second-order equations. The adsorption rate constant k_2 follows the order: CCHB3 > CCHB2 > CCHB1 > CHB, which is consistent with the experimental results. The correlation coefficient r of pseudo-second-order is greater than 0.999, much higher than the correlation coefficient r (0.925–0.974) of the pseudo-first order. The values of $Q_{e,2}$ obtained from the pseudo-second order were much closer to the actual experimental values. Thus, the pseudo-second-order model is more likely to predict the adsorption behavior of Pb^{2+} over the whole range of adsorption. Chemisorption is the

Table 1
Parameters of adsorption kinetics of the four beads (pH 4.2 at 293 K)

		Pseudo-first order			Pseudo-second order		
Adsorbent	Q_e (mmol/g)	K_1 (min^{-1})	$Q_{e,1}$ (mmol/g)	r	K_2 (g/mmol min)	$Q_{e,2}$ (mmol/g)	r
CHB	0.625	0.0149	0.334	0.974	0.0403	0.637	0.999
CCHB1	0.797	0.0060	0.513	0.967	0.0427	0.809	0.999
CCHB2	0.884	0.0137	0.742	0.945	0.0999	0.905	0.999
CCHB3	1.144	0.0150	0.979	0.925	0.1488	1.192	0.999

rate-controlling step during Pb^{2+} adsorption onto the CCHBs and CHBs [34,35].

The adsorbate can be transferred from the solution phase to the surface of the adsorbent in several steps [34], which may include external, pore, and surface diffusions as well as adsorption on the pore surface. The overall adsorption can occur through one or more steps. The intraparticle diffusion describes the process controlled by multiple diffusion mechanisms [35] and is most suitable to describe the internal diffusion dynamics of particles. The intraparticle diffusion equation is given by [36].

$$Q_t = k_{int} t^{1/2} \quad (3)$$

where Q_t is the amount of Pb^{2+} adsorbed onto cellulose and cellulose/collagen beads at time t, and k_{int} is the intraparticle diffusion rate constant (mmol/g^1 $min^{-1/2}$). The straight-line plots of Q_t against $t^{1/2}$ were used to determine the intraparticle diffusion rate k_{int} and correlation coefficient r.

Fig. 7 represents the plots of the intraparticle diffusion equation for the CCHBs and CHBs. The sharper portion is attributed to the diffusion of adsorbate through the solution to the external surface of adsorbent or the boundary layer diffusion of solute molecules or ions and represents macropore diffusion, whereas the second portion describes the gradual adsorption stage, representing micropore diffusion [36].

Table 2 shows the parameters of the intraparticle diffusion equations of the prepared biosorbents. Pb^{2+}adsorption on the CCHBs and CHBs are found to be dimerous. The first section indicates that the adsorbates diffuse to the surface of the adsorbents (film diffusion), whereas the second section demonstrates that the adsorbates diffuse to the inner intrapores (intraparticle diffusion). The first section lines of Q_t against $t^{1/2}$ is not through the origin, indicating that intraparticle diffusion is not the only step that controlled Pb^{2+}adsorption. The mass transfer rate is also controlled by pore and interior surface diffusions.

The pore structure and surface area can be used as an indicator of adsorption capacity in an adsorbent. The SEM technology was employed to observe the

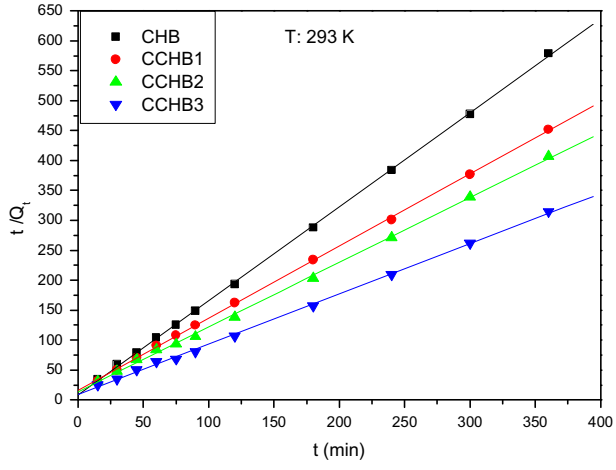

Fig. 6. Pseudo-second-order plot for Pb^{2+} adsorption onto the CCHBs and CHBs.

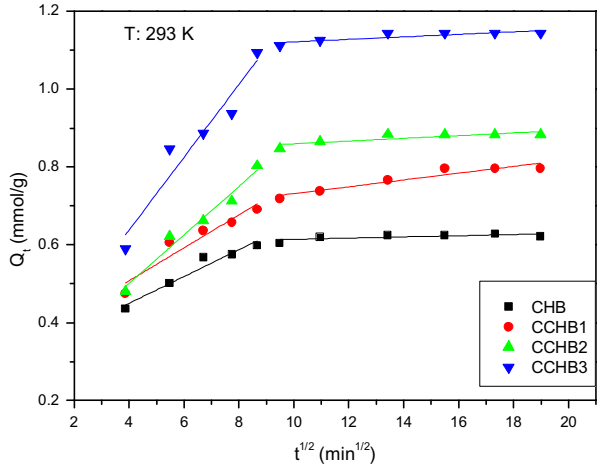

Fig. 7. Intraparticle diffusion kinetics for the adsorption of Pb^{2+} ions onto the CCHBs and CHBs.

Table 2
Parameters of intraparticle diffusion equation of the prepared biosorbents (293 K, pH 4.2, 360 min)

	Intraparticle diffusion equation			
Adsorbent	$K_{int,1}$ (mmol/g^1 min$^{-1/2}$)	r	$K_{int,2}$ (mmol/g^1 min$^{-1/2}$)	r
CHB	0.0344	0.935	0.00153	0.331
CCHB1	0.0424	0.882	0.00874	0.877
CCHB2	0.0623	0.959	0.00350	0.629
CCHB3	0.0936	0.907	0.00325	0.655

internal structure of hydrogel beads. The SEM images of cross-sections of hydrogel beads are depicted in Fig. 8. A great morphological difference between CHBs and CCHBs can be observed. CHBs show a relatively compact structure (Fig. 8(a)). CCHBs have an internal three-dimensional ultra-macroporous structure (Fig. 8(b–d), especially for CCHB3 (Fig. 8(d)). This ultra-marcoporous structure favors Pb^{2+} ions diffusion within CCHBs, which results in improving adsorption rate. It lends some support to the above results of adsorption kinetics.

N_2 adsorption can give further information of porous structure of hydrogel beads. As indicated in Table 3, the CHB, CCHB1, and CCHB3 have a specific surface area of 40.6–49.1 m^2/g except CCHB2 (25.7 m^2/g). There is no obvious influence of specific surface area on Pb^{2+} adsorption. It can be inferred that Pb^{2+} adsorption is mainly controlled by the number of active sites on adsorbents rather than specific surface area. As shown in Table 3, bulk pore volume of CHBs (85.8×10^{-3} cm^3/g) is larger than that of CCHBs ($23.4–61.1 \times 10^{-3}$ cm^3/g). Blending collagen decreases the bulk pore volume of hydrogel beads and volume quantity of meso- and macropores. It can also be observed that proportion of meso- and macropore is high for hydrogel beads (>91%), suggesting that the reconstitution of collagen or cellulose from IL solution does not facilitate micropores formation. It may one

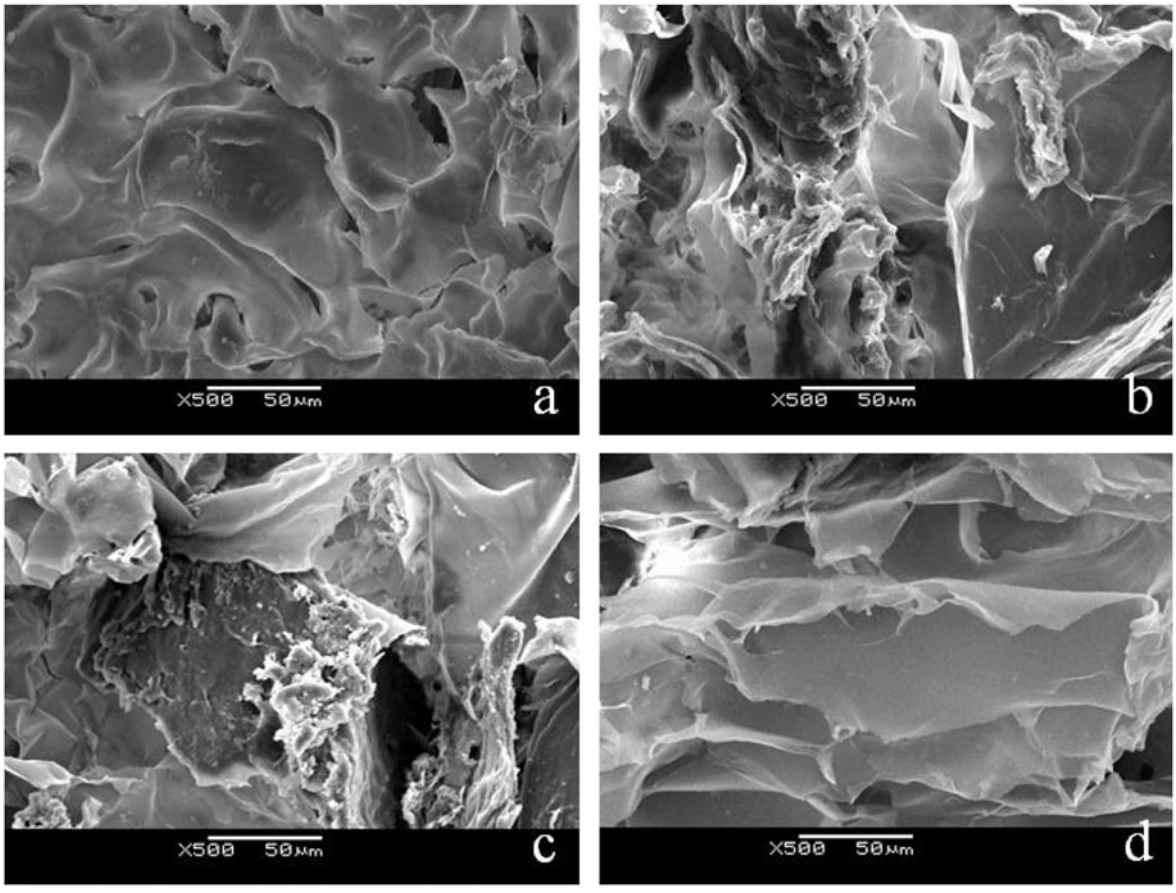

Fig. 8. SEM images of cross-sections of hydrogel beads: CHB (a), CCHB1 (b), CCHB2 (c) and CCHB3 (d).

Table 3
Specific surface area, volume quantity and proportion of different pore diameters of hydrogel beads

Adsorbent	Specific surface area (m^2/g)	Volume quantity (10^{-3} cm^3/g)			Proportion of pore diameter (%)	
		Pore diameter			Pore diameter	
		Micropore (<2 nm)	Meso-and macropore (>2 nm)	Bulk volume (10^{-3} cm^3/g)	Micropore (<2 nm)	Meso-and macropore (>2 nm)
CHB	40.6	12.2	73.6	85.8	8.2	91.8
CCHB1	25.7	4.6	18.8	23.4	2.5	97.5
CCHB2	49.1	11.9	49.2	61.1	7.4	92.6
CCHB3	44.2	13.6	30.3	43.9	8.9	91.1

be of the reasons why Pb^{2+} adsorption mainly occurs in the macropore diffusion period (first portion of plots of inparticle diffusion equation in Fig. 7).

3.3. Adsorption isotherms

In the determination of equilibrium biosorption isotherms, Pb^{2+} adsorption was investigated at varying initial concentrations ranging from 0.5 to 9.0 mmol/L at 293, 303, and 313 K under pH 4.2 and contact time of 360 min.

The influence of the initial concentration of Pb^{2+} on the adsorption capacities of CCHBs and CHBs is shown in Fig. 9. The adsorption capacities of Pb^{2+} increase with increasing initial concentration, which may have been caused by the higher concentration and fiercer competition between the Pb^{2+} ions. These phenomena cause the stronger combination between Pb^{2+} and binding sites. Thus, a higher concentration can stimulate the adsorption process. The increase in the adsorption amount is limited because of the limited binding site (Fig. 9). When Pb^{2+} concentration rises above 7.5 mmol/L for the CCHBs and CHBs, the increasing rate of adsorption capacity becomes obviously smaller, especially for the CHBs. The CCHBs may be more favorable for high concentration than the CHBs.

The equilibrium of the isotherm that described the interaction between adsorbates and adsorbents is fundamental in optimizing the use of adsorbents and essential in the design of an adsorption system. Linear Langmuir (a, c, e) and Freundlich (b, d, f) isotherms fitting Pb^{2+} adsorption onto the CCHBs and CHBs are also shown in Fig. 9.

Linear Langmuir [37] Eq. (4) and Freundlich [38] Eq. (7) isotherms were employed to analyze the adsorption characteristic in the present work using the following equations.

$$\frac{1}{Q_e} = \frac{1}{Q_{max}} + \frac{1}{Q_{max} b}\frac{1}{C_e} \tag{4}$$

$$\frac{Q_e}{C_e} = K_L Q_{max} - K_L Q_e \tag{5}$$

$$R_L = \frac{1}{1 + bC_0} \tag{6}$$

$$\ln\ Q_e = \ln\ K_f + \frac{1}{n}\ln\ C_e \tag{7}$$

where C_e and Q_e are the equilibrium concentration (mmol/L) and the amount of Pb^{2+} adsorbed at equilibrium concentration (mmol/g), respectively. Q_{max} and b are the Langmuir maximum adsorption capacity (mmol/g) and adsorption energy, respectively. K_L (obtained from Eq. (5)) is the adsorption equilibrium constant, which can preliminarily determine the adsorption type. R_L (Eq. (6)), the equilibrium parameter, can be expressed in terms of the dimensionless constant separation factor. K_f and $1/n$ are the Freundlich constant characteristics of the system, indicating the adsorption capacity and adsorption intensity, respectively.

The relevant values of the adsorption isotherms are shown in Table 4. The Langmuir isotherm is more suitable for describing Pb^{2+} adsorption onto the CCHBs and CHBs rather than the Freundlich isotherm because of the higher related coefficient r. This condition suggests that adsorption occurs at the binding sites (amino and hydroxyl groups) on the surface of the prepared hydrogel beads and follows a monolayer adsorption. Pb^{2+} adsorption onto the CHBs can be predicted using Freundlich isotherm ($r > 0.988$), contrary to the adsorption onto the CCHB3 with high collagen content. This finding indicates that the adsorption behavior of

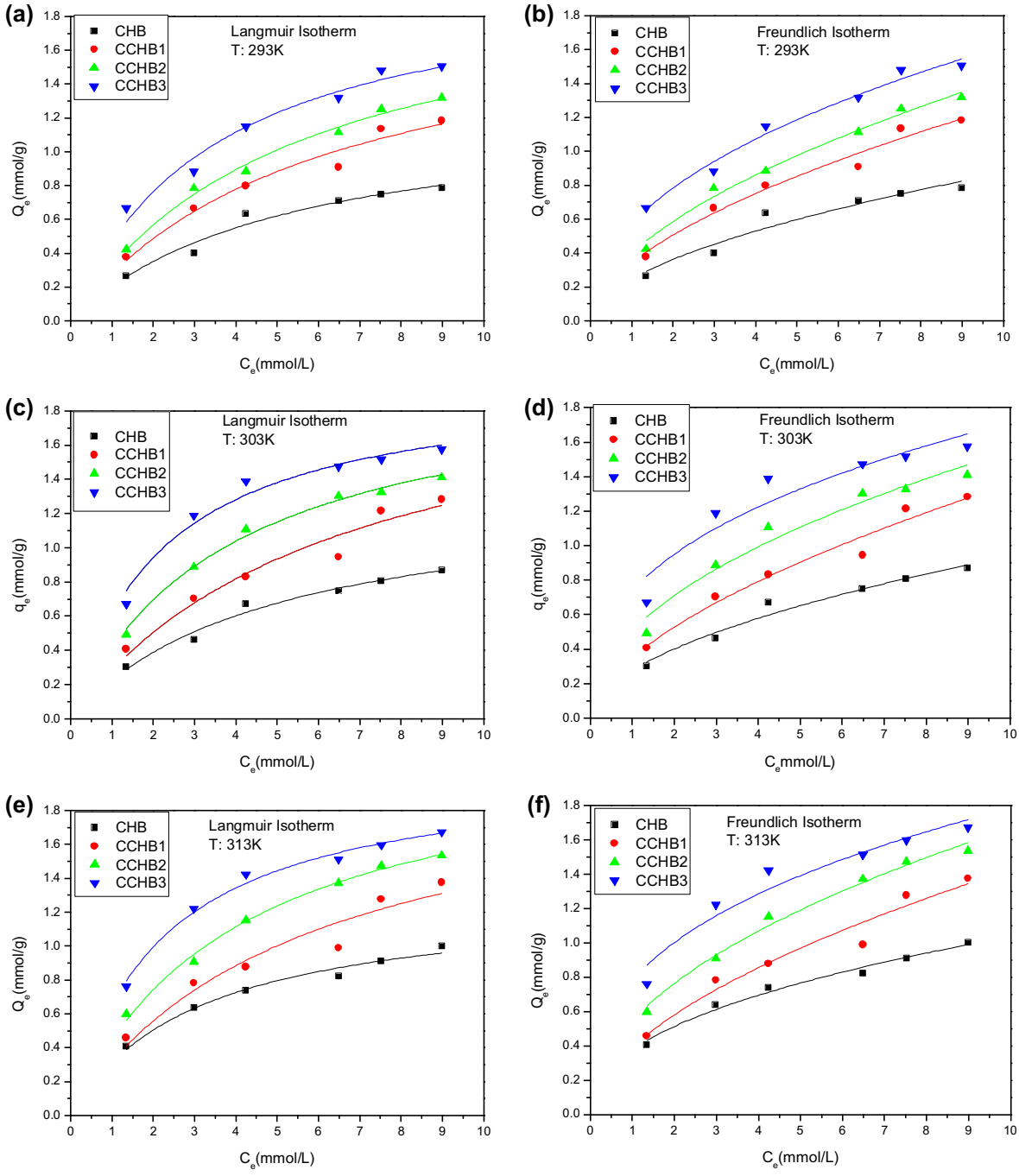

Fig. 9. Langmuir (a, c, e) and Freundlich (b, d, f) isotherms fitting Pb^{2+} adsorption onto the CCHBs and CHBs.

the hydrogel beads changes with the blending of collagen and tends to follow monolayer adsorption.

In the Langmuir isotherm, Q_{max} indicates that the binding sites are homogeneously distributed over the adsorbent surface. As depicted in Table 4, Q_{max} of Pb^{2+} are 0.856, 1.315, 1.414, and 1.598 mmol/g for CHB, CCHB1, CCHB2, and CCHB3, respectively, at 293 K. Thus, blending collagen in hydrogel beads supplies more active binding sites for Pb^{2+}. In addition, the values of R_L from this study are between 0.508 and 0.746, less than 1, indicating that the conditions used were favorable for Pb^{2+} adsorption. The value of b is closely related to the nature of the adsorbent and adsorbate. The order of b values is CCHB3 > CCHB2 > CCHB1 > CHB,

Table 4
Parameters of Langmuir and Freundlich isotherms of Pb^{2+} adsorption onto the CCHBs and CHBs

		Langmuir isotherm					Freundlich isotherm		
Adsorbent	Temperature (K)	Q_{max} (mmol/g)	b (L/mol)	K_L (mmol/g)	$R_{L,max}$	r	n	K_f ((mmol/g) $(L/mmol)^{1/n}$)	r
CHB	293	0.856	1.365	0.328	0.508	0.996	1.663	0.583	0.991
	303	1.089	1.390	0.334	0.655	0.988	1.982	0.605	0.988
	313	1.228	1.681	0.345	0.671	0.997	2.203	0.648	0.993
CCHB1	293	1.315	1.253	0.199	0.550	0.999	1.661	0.670	0.992
	303	1.486	1.450	0.350	0.622	0.991	1.809	0.675	0.986
	313	1.792	1.576	0.378	0.746	0.990	1.999	0.713	0.984
CCHB2	293	1.414	1.299	0.271	0.665	0.990	1.966	0.755	0.984
	303	1.517	1.506	0.521	0.593	0.999	2.110	0.813	0.979
	313	1.857	1.618	1.164	0.713	0.996	2.210	0.814	0.996
CCHB3	293	1.598	1.404	0.427	0.707	0.998	2.016	0.817	0.985
	303	1.833	1.857	0.521	0.463	0.994	2.491	0.871	0.939
	313	2.192	1.920	0.687	0.648	0.997	3.258	0.963	0.972

indicating that the interaction between Pb^{2+} and the biosorbents becomes stronger with increasing collagen content in the composite hydrogels.

As shown in Table 4, the values of K_L and b increase with increasing temperature, demonstrating that high temperature favors Pb^{2+} adsorption onto the CCHBs and CHBs through chelation. The data of Pb^{2+} adsorption in Fig. 8 also indicate that Q_e remarkably increases with increasing temperature. Thus, analyzing the Pb^{2+} adsorption process using thermodynamics is essential.

3.4. Adsorption thermodynamics

Thermodynamics parameters are employed to describe macroscopically the average properties of adsorbents and provide in-depth information on energy changes during the adsorption of heavy metal ions. ΔG^0 (standard free energy change, kJ/mol), ΔH^0 (standard enthalpy change, kJ/mol), and ΔS^0 (standard entropy change, [kJ/(mol K)] [39] were calculated at 293, 303, and 313 K. The standard free energy change of adsorption is given by

$$\Delta G^0 = -RT \ln K_0 \tag{8}$$

where R is the universal gas constant [8.314/(mol K)], T is the temperature in Kelvin, and K_0 is the adsorption distribution coefficient. The slope of the plot $\ln(q_e/C_e)$ vs. C_e at different temperatures yielded the adsorption distribution coefficient K_0 [40]. The relationship between ΔH^0, ΔS^0, and K_0 is as follows:

$$\ln K_0 = \frac{\Delta S^0}{R} - \frac{\Delta H^0}{RT} \tag{9}$$

The values of ΔH^0 and ΔS^0 can be obtained using the slope and intercept from the linear plot of $\ln K_0$ vs. $1/T$.

The calculated values of the thermodynamic parameters of the prepared adsorbents are shown in Table 5. The negative of ΔG^0 confirms the spontaneous nature of Pb^{2+} adsorption. The value of ΔG^0 decreases as temperature increases, demonstrating that it is favorable for the adsorption of Pb^{2+} at a high temperature. The positive ΔH^0 for Pb^{2+} adsorption confirms

Table 5
Thermodynamic parameters of Pb^{2+} adsorption onto the CCHBs and CHBs

Thermodynamic parameters	Temperature (K)	CHB	CCHB1	CCHB2	CCHB3
ΔG^0 (kJ/mol)	293	−4.361	−4.854	−3.140	−3.350
	303	−4.907	−5.670	−4.256	−4.028
	313	−5.296	−7.321	−5.561	−4.996
ΔH^0 (kJ/mol)		1.126	5.243	3.884	2.492
ΔS^0 (kJ/mol/K)		0.0056	0.0149	0.0145	0.00986

the endothermic nature of this process. Therefore, the adsorption capacity of Pb^{2+} onto the adsorbents increases with increasing temperature. Therefore, increasing the temperature is favorable for the adsorption process. The value of ΔS^0 is greater than zero, indicating that the molecular motion on the solid–liquid interface is more random.

The ΔH^0 for the CCHBs is higher than that for the CHBs, but it obviously decreases with increasing collagen content in the hydrogel beads. The order of ΔH^0 is CCHB1 (5.243 kJ/mol) > CCHB2 (3.884 kJ/mol) > CCHB3 (2.492 kJ/mol) > CHB (1.126 kJ/mol), suggesting that more energy is required during Pb^{2+} adsorption onto the composite adsorbents than that onto the cellulose adsorbents. Correspondingly, the adsorption intensity for the CCHB1 is strongest among the prepared biosorbents. The order of ΔS^0 is similar to that of ΔH^0. The degree of chaos of the solid–liquid interface on the CCHBs is higher than that on the CHBs. The blending of collagen in the hydrogel matrix increases the disorder of the binding sites on the surface of the CCHBs, but this disorder decreases with increasing collagen/cellulose mass ratio from 1:1 to 3:1. Evident difference on the interaction or distribution of collagen and cellulose in the hydrogels with varying collagen/cellulose mass ratios may exist, which greatly influence the adsorption behavior of heavy metal ions onto the prepared hydrogels. This influence is worthy of further study.

4. Conclusions

The Pb^{2+} adsorption capacity for CCHBs is higher than that for the CHBs. The optimum pH level of the solution for Pb^{2+} adsorption is 4.2. The selectivity of Pb^{2+} is higher than that of other heavy metal ions, whereas the coanions in the solution almost do not affect Pb^{2+} adsorption. Kinetic studies on adsorption of Pb^{2+} onto CCHBs reveal that the experimental data are fitted by the pseudo-second-order model, and the chemisorptions are the controlling steps. The Langmuir isotherm model has the best fit to the equilibrium experimental data by the maximum adsorption amount of 2.192 mmol/g CCHB3 at 313 K. Thermodynamic studies indicate that the adsorption process is endothermic and spontaneous. Obvious differences may exist in the interaction or distribution of collagen and cellulose in the hydrogels with varying collagen/cellulose mass ratios, which greatly influence Pb^{2+} adsorption.

Acknowledgments

The authors are grateful to the National Natural Science Foundation of China (21106011 and 21276034) and the Scientific Research Project of Department of Education of Liaoning Province (L2012195) for financial support.

References

[1] T. Depci, A.R. Kul, Y. Önal, Competitive adsorption of lead and zinc from aqueous solution on activated carbon prepared from Van apple pulp: Study in single- and multi-solute systems, Chem. Eng. J. 200–202 (2012) 224–236.
[2] S. Tong, Y.E. von Schirnding, T. Prapamonto, Environmental lead exposure: A public health problem of global dimensions, Bull. World Health Organ. 78 (2000) 1068–1077.
[3] J.C.Y. Ng, W.H. Cheung, G. McKay, Equilibrium studies of the sorption of Cu(II) ions onto chitosan, J. Colloid Interface Sci. 255 (2002) 64–74.
[4] G. Bayrammoglu, S. Bektas, M.Y. Arica, Biosorption of heavy metal ions on immobilized white-rot fungus Trametes versicolor, J. Hazard. Mater. 101 (2003) 285–300.
[5] T.P. Rao, P. Metilda, J.M. Gladis, Preconcentration techniques for uranium(VI) and thorium(IV) prior to analytical determination–An overview, Talanta 68 (2006) 1047–1064.
[6] G. Bayrammoglu, A. Denizli, S. Sektas, M.Y. Arica, Entrapment of Lentius sajor-caju into Ca-alginate gel beads for removal of Cd(VI) ions from aqueous solution: Preparation and biosorption kinetics analysis, Microchem. J. 72 (2002) 63–76.
[7] B.B. Adhikari, M. Kanemitsu, H. Kawakita, J.K. Ohto, Synthesis and application of a highly efficient polyvinyl calixarene tetraacetic acid resin for adsorptive removal of lead from aqueous solutions, Chem. Eng. J. 172 (2011) 341–353.
[8] Y.Y. Liu, Q.Q. Zhao, G.L. Cheng, H. Xu, Exploring the mechanism of lead(II) adsorption from aqueous solution on ammonium citrate modified spent Lentinus edodes, Chem. Eng. J. 173 (2011) 792–800.
[9] D. Zhou, L.N. Zhang, S.L. Guo, Mechanisms of lead biosorption on cellulose/chitin beads, Water Res. 39 (2005) 3755–3762.
[10] W.L. Yan, R.B. Bai, Adsorption of lead and humic acid on chitosan hydrogel beads, Water Res. 39 (2005) 688–698.
[11] N. Li, R.B. Bai, Highly enhanced adsorption of lead ions on chitosan granules functionalized with poly(acrylic acid), Ind. Eng. Chem. Res. 45 (2006) 7897–7904.
[12] L.V.A. Gurgel, L.F. Gil, Adsorption of Cu(II), Cd(II), and Pb(II) from aqueous single metal solutions by succinylated mercerized cellulose modified with trithylenetetramine, Carbohydr. Polym. 77 (2009) 142–149.
[13] L.X. Zhong, X.W. Peng, D. Yang, R.C. Sun, Adsorption of heavy metals by porous bioadsorbent from lignocel-

lulosic biomass reconstructed in an ionic liquid, J. Agric. Food Chem. 60 (2012) 5621–5628.
[14] X.Q. Sun, B. Peng, Y. Ji, J. Chen, D.Q. Li, Chitosan(chitin)/cellulose composite biosorbents prepared using ionic liquid for heavy metal ions adsorption, AIChE J. 55 (2009) 2062–2069.
[15] R.X. Liu, J.L. Guo, H.X. Tang, Adsorption of fluoride, phosphate, and arsenate ions on a new type of ion exchange fiber, J. Colloid Interface Sci. 248 (2002) 268–274.
[16] F.H. Silver, J.W. Freeman, G.P. Seehra, Collagen self-assembly and the development of tendon mechanical properties, J. Biomech. 36 (2003) 1529–1553.
[17] Z.J. Meng, X.J. Zheng, K.Y. Tang, J. Liu, Z. Ma, Q.L. Zhao, Dissolution and regeneration of collagen fibers using ionic liquid, Int. J. Biol. Macromol. 51 (2012) 440–448.
[18] R.P. Swatloski, S.K. Spear, J.D. Holbrey, R.D. Rogers, Dissolution of cellulose with ionic liquids, J. Am. Chem. Soc. 124 (2002) 4974–4975.
[19] H.F. Wang, H.N. Lv, J. Feng, Z.K. Wang, Novel blend films prepared from solution of collagen and cellulose in 1-allyl-3-methylimizolium chloride ionic liquid, Adv. Mater. Res. 418–420 (2012) 30–33.
[20] Z.J. Cai, G. Yang, Bacterial cellulose/collagen composite: Characterization and first evaluation of cytocompatibility, J. Appl. Polym. Sci. 120 (2011) 2938–2944.
[21] Y.M. Zhao, X.L. Hu, J.Y. Yu, P. Guan, Preparation of polysulfone membranes using ionic liquid [C][SCN] as a pore-former and plasticizer, Adv. Mater. Res. 87–88 (2010) 74–79.
[22] J.L. Wang, M.H. Li, L.G. Wei, Y.C. Ma, K.L. Li, Y.C. Yu, Cellulose/collagen beads prepared using ionic liquid for Cu(II) adsorption from aqueous solutions, Adv. Mater. Res. 535–537 (2012) 2365–2369.
[23] S.P. Yang, S.Y. Fu, H. Liu, Y.M. Zhou, X.Y. Li, Hydrogel beads based on carboxymethyl cellulose for removal heavy metal ions, J. Appl. Polym. Sci. 119 (2011) 1204–1210.
[24] B. Ozkahraman, I. Acar, S. Emik, Removal of Cu^{2+} and Pb^{2+} ions using CMC based thermoresponsive nanocomposite hydrogel, Clean Soil, Air, Water 39 (2011) 658–664.
[25] J.G. Huddleston, A.E. Visser, W.M. Reichert, H.D. Willauer, G.A. Broker, R.D. Rogers, Characterization and comparison of hydrophilic and hydrophobic room temperature ionic liquids incorporating the imidazolium cation, Green Chem. 3 (2001) 156–164.
[26] D.L. Zhang, Y.F. Deng, C.B. Li, J. Chen, Separation of ethyl acetate-ethanol azeotropic mixture using hydrophilic ionic liquids, Ind. Eng. Chem. Res. 47 (2008) 1995–2001.
[27] D. Zhou, L.N. Zhang, J.P. Zhou, S.L. Guo, Cellulose/chitin beads for adsorption of heavy metals in aqueous solution, Water Res. 38 (2004) 2643–2650.
[28] M. Ozacar, I.A. Sengil, H. Turkmenler, Equilibrium and kinetic data, and adsorption mechanism for adsorption of lead onto valonia tannin resin, Chem. Eng. J. 143 (2008) 32–42.
[29] R. Laus, V.T. de Favere, Competitive adsorption of Cu (II) and Cd(II) ions by chitosan crosslinked with epichlorohydrin–triphosphate, Bioresour. Technol. 102 (2011) 8769–8776.
[30] S.C. Tsai, T.H. Wang, Y.Y. Wei, W.C. Yeh, Y.L. Jan, S.P. Teng, Kinetics of Cs adsorption/desorption on granite by a pseudo first order reaction model, J. Radioanal. Nucl. Chem. 275 (2008) 555–562.
[31] S. Larous, A.H. Meniai, M.B. Lehocine, Experimental study of the removal of copper from aqueous solutions by adsorption using sawdust, Desalination 185 (2005) 483–490.
[32] Y.S. Ho, G. McKay, The sorption of lead(II) ions on peat, Water Res. 33 (1999) 578–584.
[33] Y.S. Ho, G. Mckay, Pseudo-second order model for sorption processes, Process Biochem. 34 (1999) 451–465.
[34] Y. Onal, C. Akmil-Basar, D. Eren, C. Sarc-Ozdemir, T. Depci, Adsorption kinetics of malachite green onto activated carbon prepared from Tuncbilek lignite, J. Hazard. Mater. B 128 (2006) 150–157.
[35] W.S. Wan Ngah, S. Fatinathan, Adsorption of Cu(II) ions in aqueous solution using chitosan beads, chitosan-GLA beads and chitosan-alginate beads, Chem. Eng. J. 143 (2008) 62–72.
[36] M.S. Chiou, H.Y. Li, Adsorption behavior of reactive dye in aqueous solution on chemical cross-linked chitosan beads, Chemosphere 50 (2003) 1095–1105.
[37] I. Langmuir, The constitution and fundamental properties of solids and liquids. Part I. Solids, J. Am. Chem. Soc. 38 (1916) 2221–2295.
[38] H.M.F. Freundlich, Uber die adsorption in losungen [About the adsorption in solutions], Z. Phys. Chem. 57 (1906) 385–470.
[39] Y. Khambhaty, K. Mody, S. Basha, B. Jha, Kinetics, equilibrium and thermodynamic studies on biosorption of hexavalent chromium by dead fungal biomass of marine Aspergillus niger, Chem. Eng. J. 145 (2009) 489–495.
[40] A.A. Khan, R.P. Singh, Adsorption thermodynamics of carbofuran on Sn(IV) arsenosilicate in H^+, Na^+ and Ca^{2+} forms, Colloids Surf. 24 (1987) 33–42.